NRIAG JOURNAL OF ASTRONOMY AND GEOPHYSICS
2021, VOL. 10, NO. 1, 93–109
https://doi.org/10.1080/20909977.2021.1880817

Taylor & Francis
Taylor & Francis Group

ARTICLE

OPEN ACCESS Check for updates

Aeromagnetic interpretation of basement structure and architecture of the Dahomey Basin, Southwestern Nigeria

Okoro E. Martins, Onuoha K. Mosto and Oha A. Ifeanyi

Department of Geology, University of Nigeria Nsukka, Enugu, Nigeria

ABSTRACT

Significant yet untapped resources still abound in the Nigerian sector of the Dahomey Basin. Although the presence of an extensive Cretaceous Petroleum System has been confirmed following recent discoveries in Aje and Ogo Fields offshore Lagos, exploration outputs in the Dahomey Basin has so far not been encouraging. Proper understanding of the basement architectural framework and controls on tectonic development remains key to unlock the unrealised potentials in the basin. Hence, a geophysical interpretation of the basement structure and architecture of the Dahomey Basin southwestern Nigeria has been carried out in this study. Various edge enhancement techniques were applied to the high-resolution residual magnetic intensity (HRRMI) grid of the area. This includes first vertical derivative (FVD), total horizontal derivative (THDR), tilt derivative (TDR) and total horizontal derivative of upward continuation (10 km). Determination of the depth to magnetic sources and sedimentary thicknesses in the study area were achieved using standard Euler deconvolution and source parameter imaging (SPI) techniques, with depth range of 4.5–6.3 km attained in the two identified sub-basins located offshore of the study area. Lineament analysis gave insights on the tectonic trends and stress-field orientation in the basin with major trends in the NNE-SSW, NE-SW, NW-SE, and WNW-ESE directions. 2D forward modelling of some selected profiles was employed to characterise the basement pattern and architecture, which depicted a horst-graben architecture. The basement structure and architecture have a major control on the distribution of sub-basins, petroleum systems elements and trap styles in the basin. The study demonstrates the robust application of high-resolution aeromagnetic data in basin-wide mapping of regional subsurface geological features, basement architecture and determination of sedimentary thickness in a frontier basin.

ARTICLE HISTORY
Received 18 August 2020
Revised 2 January 2021
Accepted 19 January 2021

KEYWORDS
Aeromagnetic data; basement structure; basement architecture; dahomey Basin

1. Introduction

The Dahomey Basin is a narrow E-W trending strip of coastal/inland basin with a significant offshore component. It stretches from southeastern Ghana through southern Togo and Benin Republic and terminates at the Okitipupa ridge in Southwestern Nigeria. The Nigerian sector of the Dahomey Basin, is known for its large bitumen and heavy oil deposits, however, there are indications that the basin possesses enormous potential for hydrocarbon which are grossly underexplored. An estimated (prospective and proven) reserve of up to 15–20 billion barrels of oil equivalent have been reported (e.g. Omatsola 2019; Ladipo and Lipede 2019). Recent exploration successes in the Aje and Ogo Fields offshore Lagos have confirmed the presence of an extensive Cretaceous Petroleum System in the area. Moreover, the basin is yet to yield expected exploration results after witnessing several failed drilling campaigns in the onshore and shallow shelf areas for many decades (Adeoye et al. 2013; Ladipo and Lipede 2019). The Late Jurassic rifting phase initiated transcurrent movements along oceanic transform faults and controlled the development of marginal basins along the West African coast, including the Dahomey Basin (Omatsola and Adegoke 1981; Mascle et al. 1988; Burke et al. 2003; Brownfield and Charpentier 2006). Proper understanding of the basement architectural geometry in relation to the tectonic development of the Gulf of Guinea remains key to unlock the undiscovered potentials and increase exploration success in the Dahomey Basin (Opara et al. 2012; Oladele and Ayolabi 2014).

Aeromagnetic data interpretation enables enhanced tectonic framework characterisation of frontier basins by providing information on the regional distribution of shallow and deep-seated structural features in basin domains (Li and Morozov 2015). Generally, sedimentary basins are associated with low magnetic signals due to low magnetic susceptibility sediments in them. Hence, mapping the sediment–basement interface images the basement topography and provides information about the thickness of the overlying sedimentary successions, including deep-seated regional geological features, basement types, blocks and near-surface lineaments (Li and Morozov 2015; Oladele

CONTACT Oha A. Ifeanyi ifeanyi.oha@unn.edu.ng Department of Geology, University of Nigeria Nsukka, Enugu, Nigeria

© 2021 The Author(s). Published by Informa UK Limited, trading as Taylor & Francis Group.
This is an Open Access article distributed under the terms of the Creative Commons Attribution License (http://creativecommons.org/licenses/by/4.0/), which permits unrestricted use, distribution, and reproduction in any medium, provided the original work is properly cited.

et al. 2016). In combination with seismic data, these viable geophysical tools can open-up new opportunities in the Dahomey Basin by providing enhanced images of the subsurface for accurate determination of basement depth, basement block pattern and enhanced tectonic framework modelling (Oladele et al. 2015; Tyrrell et al. 2017; Okoro and Onuoha 2019).

Many researchers have attempted to characterise the structural and tectonic features of the Dahomey Basin using various geophysical methods (e.g., Opara et al. 2012; Oladele and Ayolabi 2014; Oladele et al. 2015, 2016). However, little attention has been paid to the evaluation of the controls that basement architecture may have on the distribution of petroleum systems elements across the basin. More recently, Tyrrell et al. (2017) and Babangida et al. (2019) provided evidence from 3D seismic dataset that the regional distribution of Lower Cretaceous sediments in half-graben structures offshore Dahomey Basin were controlled by strike-slip deformations associated with movements along oceanic fracture zones.

The present study provides additional insights on the basement block faults and architecture of the Dahomey Basin through structural interpretation of aeromagnetic data and sheds more light on the existence of sub-basins with thick sedimentary packages for further targeting and concentration of exploration efforts.

2. Location of study and geological setting

The Nigerian sector of the Dahomey Basin is located within the Gulf of Guinea (Figure 1) and covers the southwestern part of Nigeria between longitudes 2° 30′E and 5°00′E, and latitudes 6°00′N and 7°00′N, cutting across three different states including Lagos, Ogun and Ondo States. The northern edge of the basin is defined by the Basement Complex rocks of southwestern Nigeria, which is part of the West African Shield (Rahaman 1976; Oluyide 1988). To the east, it is limited by the Okitipupa Ridge (supposedly a continental extension of the Chain Fracture Zone) which forms a wedge that separates its Cretaceous – Cenozoic sediments from the Tertiary sediments of the Niger Delta. The Dahomey basin extends westerly through Benin and Togo into Ghana where the boundary is defined by the Ghana Ridge (supposedly a continental extension of the Romanche Fracture Zone). The southern limit is the Atlantic Ocean. As part of the West African peri-cratonic basin system (Guiraud and Maurin 1992; Burke et al. 2003; Bumby and Guiraud 2005; Brownfield and Charpentier 2006), the Dahomey Basin covers much of the continental margin of the Gulf of Guinea.

Tectonic evolution of the Dahomey Basin has been related to the Late Jurassic transcurrent movements along oceanic fractures zones which resulted in the opening-up of the South Atlantic and subsequent separation of the African and South American Plates (Omatsola and Adegoke 1981; Mascle et al. 1988; Onuoha and Ofoegbu 1988; Brownfield and Charpentier 2006; Omosanya et al. 2012; Kaki et al. 2013; Fadiya and Ojoawo 2015). Basement tectonics and block faulting comprised the intra-cratonic (pre-drift), syn-rift (or rift) and post-rift (drift) stages which resulted in the formation of east to west oriented structural basins. The boundaries of each of these structural basins are defined by the east – west transform fault systems (Akande et al. 2012). Hence, the observed principal basement structures in the basin are related to Early Cretaceous rifting, dominated by normal faults bounding a series of linked half-grabens. The major structures appear to have formed in the Neocomian to Barremian (Oladele and Ayolabi 2014).

The general geology (Figure 2) and tectonostratigraphic sequences of the Dahomey Basin which span from Cretaceous to Recent, and have been studied extensively by many researchers (e.g., Adekeye et al. 2019; Omatsola and Adegoke 1981; Billman 1992; Jan Duchene 1998; Omosanya et al. 2012; Kaki et al. 2013; d'Almeida et al. 2016; Akande et al. 2018). This includes the Cretaceous Abeokuta Group, which comprise the Ise, Afowo and Araromi Formations; the Palaeocene Ewekoro Formation; the Late Palaeocene to early Eocene Akinbo Formation; the Eocene Oshosun and Ilaro Formations and the Pleistocene to Recent Benin Formation (Figure 3).

3. Materials and methods

3.1. Aeromagnetic data

The Nigerian sector of the Dahomey Basin is covered by an aeromagnetic survey conducted by the Nigerian Geological Survey Agency (NGSA) between December 2006 and May 2007. Acquisition of the high-resolution aeromagnetic data was carried out by Fugro Airborne Survey Limited, using 3 x Scintrex CS3 Caesium Vapour Magnetometers which samples at 0.1 second and records Total Magnetic Intensity (TMI) data at 0.001nT resolution. The airborne magnetic surveys were flown at 80 m terrain clearance along a series of equally spaced parallel flight lines (500 m apart) which trend 135 degrees. The geomagnetic gradient was removed from the data using the International Geomagnetic Reference Field (IGRF) formula for 2005. Upon acquisition, the aeromagnetic data were pre-processed and reduced to a format that will enable direct relationship with the subsurface

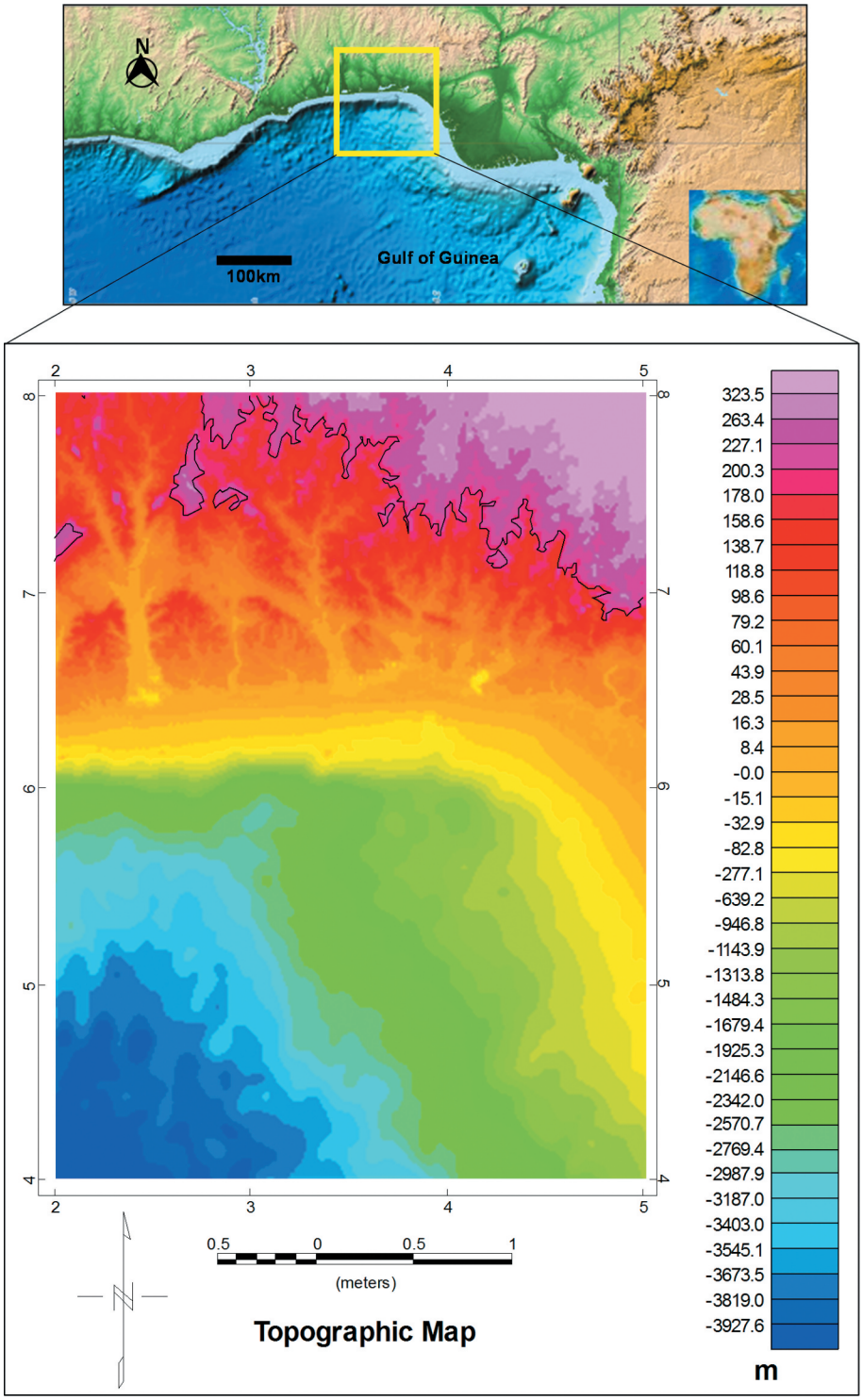

Figure 1. Relief Map of the Gulf of Guinea showing location of the study area in yellow box and Gridded Topographic (Etopo1) Image of the Nigeria's Portion of the Dahomey Basin.

geology to be established. Pre-processing operations on the newly acquired data include micro-levelling, deculturing to reduce noise content, and minimising mis-tie and removing cultural effects resulting from metallic features (e.g. pipelines, railways, steel tower, etc.). This was succeeded by data interpolation into rectangular grids with 125 m cell size (equivalent to a quarter of the flight line spacing) using a minimum curvature algorithm with a constant elevation of 80 m. The end product of this process is the total magnetic intensity (TMI) map. Each TMI grid is presented on a scale of 1:100,000 and half degree sheet, covering an area of about 3025 km^2.

Ten high-resolution aeromagnetic data grids (sheets: 278, 279, 280, 281, 282, 278A, 279A, 280A, 281A and 296) covering the study area were made available by the NGSA. These aeromagnetic grids were merged to obtain a single TMI grid (Figure 4), with a total field strength of 32,621.407nT and average inclination and declination of −12.84° and −3.37°,

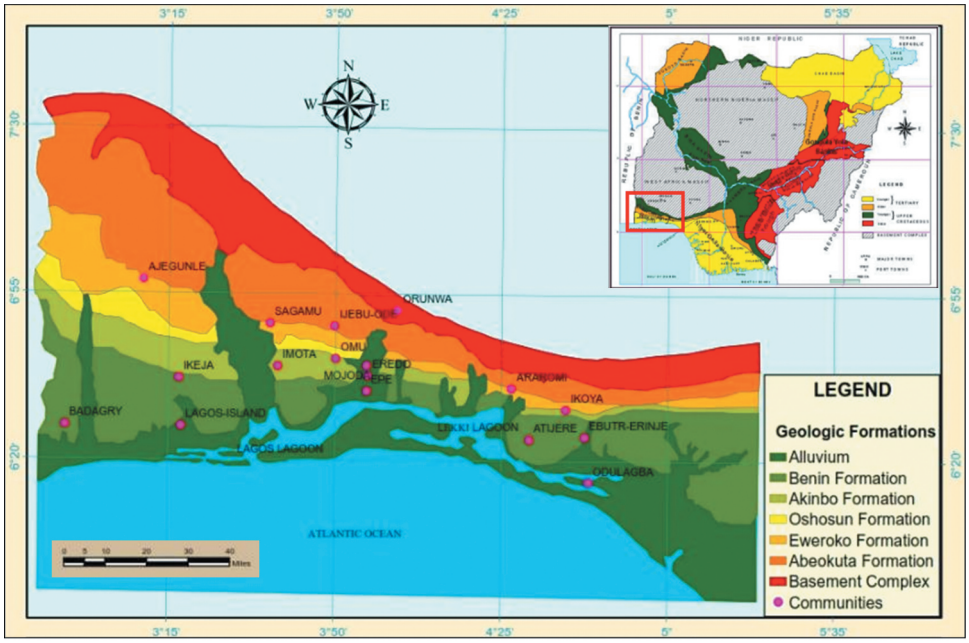

Figure 2. Geological Map of Nigeria's Portion of the Dahomey Basin (modified after Adekeye et al., 2019).

GEOLOGIC TIME		FORMATION			
PERIOD	EPOCH	Ako et al. (1980)	Omatsola and Adegoke (1981)	Billman (1992)	
QUATERNARY	HOLOCENE PLEISTOCENE	Coastal Plain Sands	Benin Fm	Benin Fm	POST-RIFT
TERTIARY	EOCENE	Ilaro Fm	Ilaro Fm	Ijebu Fm	
		Oshosun Fm	Oshosun Fm	Oshosun Fm	
	PALEOCENE	Ewekoro Fm	Ewekoro Fm	Imo Shale	
CRETACEOUS	MAASTRICTIAN CAMPANIAN	Abeokuta Fm	Abeokuta Group: Araromi Fm	Nkporo Shale	
	CONIACIAN TURONIAN		Abeokuta Group: Afowo Fm	Awgu Fm	
	CENOMANIAN			Abeokuta Fm	
	BARREMIAN		Abeokuta Group: Ise Fm	Folded Sediments	SYN-RIFT

Figure 3. Generalised Stratigraphic Chart of the Eastern Dahomey Basin (modified after Adekeye et al., 2019; Akande et al. 2018).

respectively. The total area covered is approximately 30,250 km^2. The white portions on the merged TMI map of the study area signify missing data sections corresponding with Lagos metropolis where no data was acquired. The TMI data formed the basis for further application of enhancement filters for detailed analysis and interpretation of the study area.

3.2. Aeromagnetic data analysis

High-resolution aeromagnetic data processing and enhancements started with reducing the TMI grid to the magnetic equator. Reduction to the equator (RTE) filter removes the asymmetric nature of the anomalies associated with magnetic data at low latitudes (less than 15°) and reconstructs them so that the magnetic

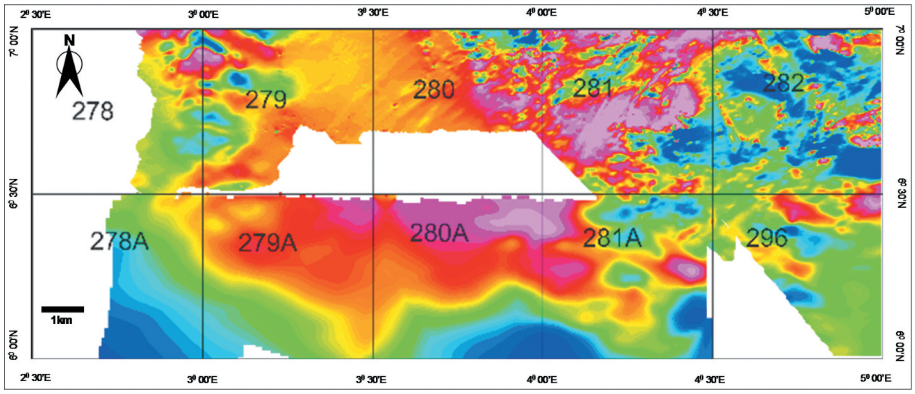

Figure 4. Merged aeromagnetic grid showing the ten data sheets used in this study.

anomalies are symmetrically centred over their causative sources (Blakely 1995; Geosoft 2015). The RTE map of the study area was produced using geomagnetic inclination and declination of −12.84°and −3.37°, respectively. Upward continuation filter was used to smoothen the RTE data by attenuating short-wavelength anomalies and enhancing deep-seated regional features related to long-wavelength anomalies (Blakely 1995). The residual magnetic intensity (RMI) grid was then computed by subtracting the upward continued (5 km) grid from the original RTE grid.

3.2.1. Edge enhancement techniques

Edge enhancement filters used in this study to define contact locations include first vertical derivative (FVD), total horizontal derivative (THDR), tilt derivative (TDR) normalised by upward continuation to 1 km and total horizontal derivative of upward continuation (10 km). Analysis of the extracted lineaments using rose diagrams gave clue on the dominant tectonic trends and stress-field directions in the study area.

A detailed description of the theory and applications of these methods have been given in classical literatures (e.g. Thompson 1982; Roest et al. 1992; Thurston et al. 1999; Nabighian et al. 2005; Reeves 2005). However, these routines are briefly outlined here.

3.2.1.1. First vertical derivative (FVD). This enhancement filter calculates the vertical rate of change in the magnetic signal (Milligan and Gunn 1997). It emphasises short-wavelength anomalies associated with shallow geological structures. Mathematically, the first vertical derivative (Phillips 2000) is given by the equation:

$$FVD = -\frac{\partial F}{\partial Z} \quad (1)$$

It is a good filter for delineating near-surface contacts and lineaments.

3.2.1.2. Total horizontal derivative (THDR). The THDR (Cordell and Grauch 1985) is a common edge detection filter for delineating shallow linear structures (faults and contacts). It is defined as:

$$TDHR = \sqrt{\left(\frac{\partial M}{\partial x}\right)^2 + \left(\frac{\partial M}{\partial y}\right)^2} \quad (2)$$

where (∂M/∂x) and (∂M/∂y) are the horizontal derivatives of the magnetic field. Discontinuities in the N – S direction are accentuated by the x component of the derivative, while the y component acts in a similar way to contacts in the E – W direction. In general, the total horizontal derivative anomaly generated by a tabular body tends to overlie the edges of the anomalous body, whether vertical or horizontal and separated from each other (Cordell and Grauch 1985). The THDR has low sensitivity to noise in the data since it only requires computation of the first horizontal derivatives of the field in x and y directions (Cooper and Cowan 2008). The THDR maxima were employed in this study to delineate edges of shallow linear features such as faults and fracture networks.

3.2.1.3. Tilt derivative (TDR). The tilt derivative (Miller and Singh 1994; Oruç and Keskinsezer 2008) filter is given by the arctangent of the ratio of the vertical derivative of the potential field to its total horizontal derivative:

$$TDR = tan^{-1}\left(\frac{VDR}{THDR}\right) \quad (3)$$

The technique is considered as a powerful method for detecting the edges of causative sources and for mapping shallow basement structures (Shahverdi et al. 2017; Ibraheem et al. 2018). The range of variation of the tilt derivative amplitude is between -π/2 and π/2; positive values are located over the sources, zero values at/near the source edge and negative values are located away from the source (Verduzco et al.

2004; Ibraheem et al. 2018). Enhancement filters that boost subtle (short wavelength) anomalies also exacerbate the short-wavelength noise, which needs to be suppressed before applying the filter (Lyatsky et al. 2005). In this study, noise suppression was achieved by slightly upward continuing the RTE data by 1 km before computing the TDR grid.

3.2.1.4. Upward continuation (UC). This mathematical technique transforms the magnetic data by calculating the field at constant elevation (h) above the plane of measurement (Pacino and Introcaso 1987). The upward continuation filter attenuates noise in the data, removes the effects of shallow sources and emphasises long-wavelength anomalies associated with deep-seated regional features in the survey area (McCurry 1970). The upward continued (ΔF) of the total field anomaly at higher elevation (z = -h) is given by:

$$\Delta F(x,y,-h) = \frac{h}{2\pi}\int \frac{\Delta F(x,y,0)dxdy}{\left((x-x^0)^2+(y-y^0)^2+h^2\right)}\ldots \quad (4)$$

According to and Mekonnen (2004), the equation (5) gives the field at an elevation (h) above the plane of the observed field (z = 0) in terms of the average value ΔF at the point (x, y, o).

The RTE grid was upward continued to 10 km above the survey plane to obtain the regional anomaly map. Total horizontal derivative (THDR) of the upward continued grid was then computed in order to map the deep-seated regional structures in the study area.

3.2.2. Depth estimation methods

Depths to causative anomalous bodies were determined using standard Euler deconvolution and source parameter imaging (SPI) methods, while 2D forward modelling of some selected profiles, performed with the GM-SYS™ module of Oasis Montaj software, gave insights on the basement block pattern and architecture.

The depth estimation methods are briefly described as follows.

3.2.2.1. Source parameter imaging (SPI). The source parameter imaging (SPI) technique (Thurston and Smith 1997; Thurston et al. 1999) or the local wavenumber method (Smith et al. 1998) is based on the principle of complex analytic signal which computes source parameters from gridded magnetic data. This method requires computation of the first- and second-order derivatives, making it susceptible to noise and interference effects (Nabighian et al. 2005). The basics is that for vertical contacts, the peaks of the local wavenumber define the inverse of depth. Hence, the depth is calculated using the formula:

$$Depth = \frac{1}{K_{max}}\ldots \quad (5)$$

where K_{max} is the peak value of the local wavenumber K over the steep source. The wavenumber is given by the expression:

$$K_{max} = \sqrt{\left(\frac{\partial Tilt}{\partial x}\right)^2 + \left(\frac{\partial Tilt}{\partial y}\right)^2}\ldots \quad (6)$$

SPI solution grids show the susceptibility contrasts, depths, edge locations and dips of magnetic source bodies. Therefore, SPI map more closely resembles the geology, giving a better image of the basement–sediment interface than either the original magnetic data or its derivatives. The technique is best suited for isolated 2D sources such as contacts, thin sheet edges, or horizontal cylinders (Nabighian et al. 2005). The SPI method was used in this study to determine the depth to anomalous causative bodies and to map the basement topography.

3.2.2.2. Standard Euler deconvolution. The standard Euler deconvolution (Thompson 1982) is based on Euler's homogeneity equation (Reid et al. 1990):

$$(x-x_0)\frac{\partial T}{\partial x} + (y-y_0)\frac{\partial T}{\partial y} + (z-z_0)\frac{\partial T}{\partial z} = N(B-T)\ldots \quad (7)$$

where x_0, y_0, z_0 is the position of the magnetic body, T is the total field measured at (x, y, z), B is regional value of the magnetic field and N is the structural index. The Euler deconvolution relates the potential field and its gradient components to the location of the sources, by the degree of homogeneity N. The method enables estimation of source location and depth, including contacts like the faults and other sharp structural contrasts based on different geological models replicating dikes, sills, pipes and horizontal cylinders. A structural index of 0.5 and 1 was used in this study.

4. Results and discussions

4.1. Aeromagnetic signatures of the Dahomey Basin

Colour-shaded images of the TMI map (Figure 5), RTE map (Figure 6) and RMI map (Figure 7) shows a variation in the magnetisation of the different rocks underlying the study area. These were manifested as high, low and intermediate anomalies trending in the NE-SW, NW-SE, N-S, WNW-ESE and E-W directions. The TMI map shows dominance of the high anomaly values from 50.9 to 106.6nT within the central portion

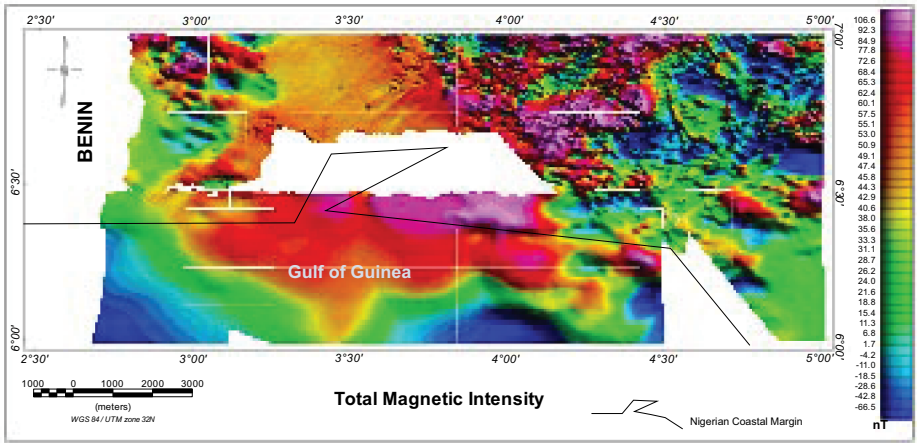

Figure 5. Total magnetic intensity map of the study area.

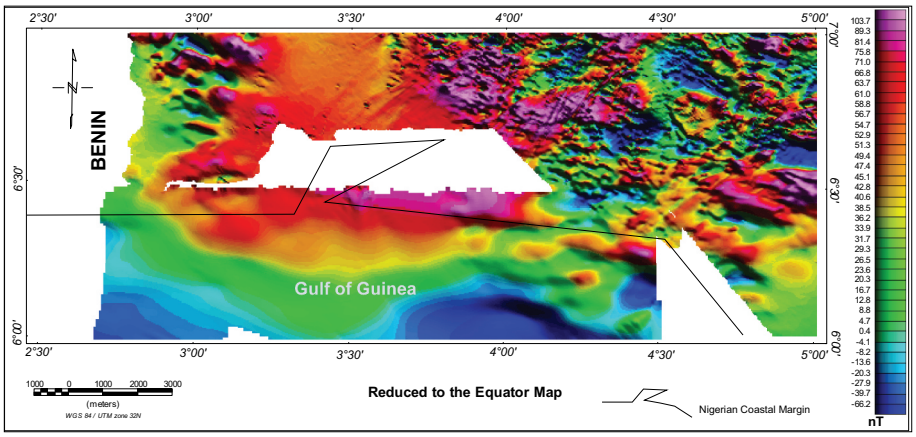

Figure 6. Reduced to the Equator map of the study area.

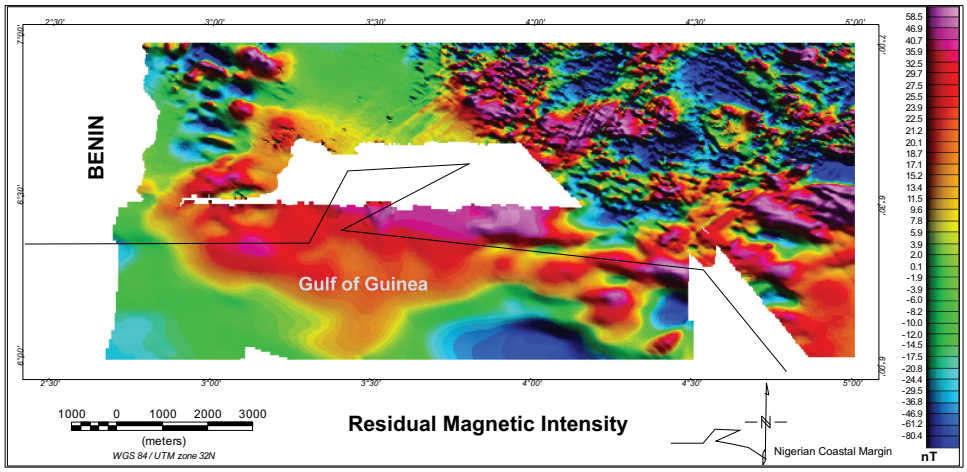

Figure 7. Residual magnetic intensity map of the study area.

of the map, while low anomalies between −4.2 and −66.5nT dominate the northeastern part, as well as the southern and southwestern portions beyond the Nigerian coastal margin. Intermediate anomalies (11.3–42.9nT) drape the positive and negative anomalies all over the map.

Like the TMI map, high magnetic anomaly values from 49.4 to 103.7nT were also observed at the central,

and parts of the eastern, portion of the RTE map; while low anomalies between −4.1 and −66.2nT are located in southern, southwestern and parts of the northeastern portions. Intermediate anomalies ranging from 4.6 to 47.4nT dominate the southeastern and parts of the northeastern and central portions of the study area.

The RMI map is somewhat different from the TMI and RTE maps in that intermediate anomalies (−17.-5–3.9nT) dominate the northern part of the central portion, as well as the southwestern portion of the map. Positive anomalies ranging from 7.8 to 58.5nT characterise the southern part of the central and southeastern portions of the map, while low anomaly responses (−80.4 to −20.8nT) are located within the northeastern and southern portions of the map. The anomalies exhibit sharp magnetic boundaries, which are typical of vertical or steeply dipping contacts (faults). In general, aeromagnetic signatures of the study area reflect strong anomalous features of different amplitudes and sizes that trends nearly parallel to the basin configuration.

The high and low anomalous zones are separated from each other by steep gradients, reflecting the edges of magnetic sources (Oladele et al. 2015). The linear nature of these magnetic gradients suggests they might be structures associated with block faulting which are responsible for the rugose nature of the underlying basement rocks (Okoro and Onuoha 2019). The magnetic highs and lows are closely related to the major geological features in the basin. For instance, the high magnetic anomaly that extends beyond the Nigerian coastal margin is considered the marginal ridge that marks the continent-ocean boundary within the Gulf of Guinea (Gaina et al. 2013); while the low magnetic anomalies beyond the Nigerian coastal margin correlates with graben features where the basement block has dropped to considerable depths, allowing the accumulation of thick sedimentary packages.

4.2. Structural style of the Dahomey Basin

The structural geometry of the Dahomey Basin was established based on integration of all the results obtained after applying various enhancement filters to the aeromagnetic data to map the basement at depth (Teasdale et al. 2001). The interpreted near-surface and deep-seated structures show evidence of wrench tectonics, with conjugate sinistral and dextral displacements reflecting the imprints of transcurrent motions along oceanic transform faults which controlled the development of the faults. Major trends of the faults are in the NNE-SSW, NE-SW, NW-SE and WNW-ESE directions, respectively. The faults and fractures are well displayed on the total horizontal derivative map (Figure 8) of the study area and were responsible for fragmenting the basement into several blocks of different magnetic susceptibilities, giving it a rugose horst-graben architecture (Adekeye et al. 2019; Onuoha and Ofoegbu 1988; Oladele and Ayolabi 2014; Oladele et al. 2016; Okoro and Onuoha 2019). These structures generally influenced the distribution of sub-basins, petroleum systems elements, trap styles, hydrocarbon migration and other resources in the basin.

4.2.1. Near-surface structures

The shallow linear features identified on the FVD map (Figure 9) and TDR map (Figure 10) include faults and fractures systems with different orientations. Linear features from the FVD map showed major and minor trends in the NW-SE and NE-SW directions, while the observed major and minor trends on the TDR map include NNE-SSW and WNW-ESE directions, respectively. The FVD

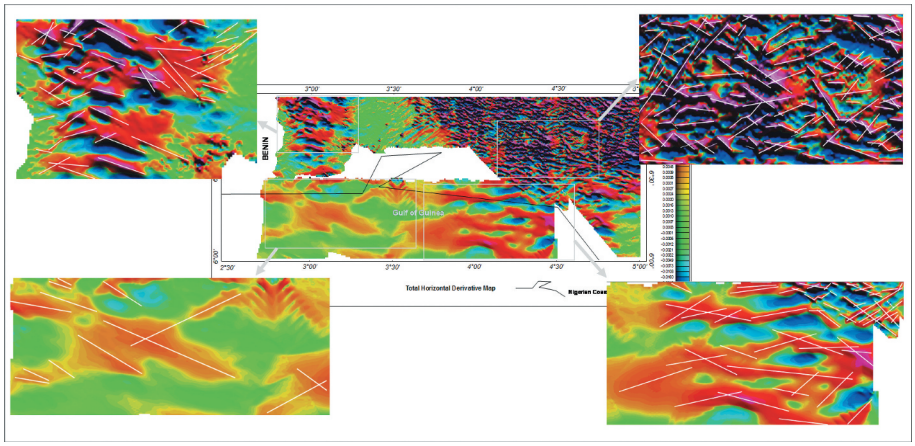

Figure 8. Total horizontal derivative map showing structural style of the study area; the rose diagram shows major trends of the linear features.

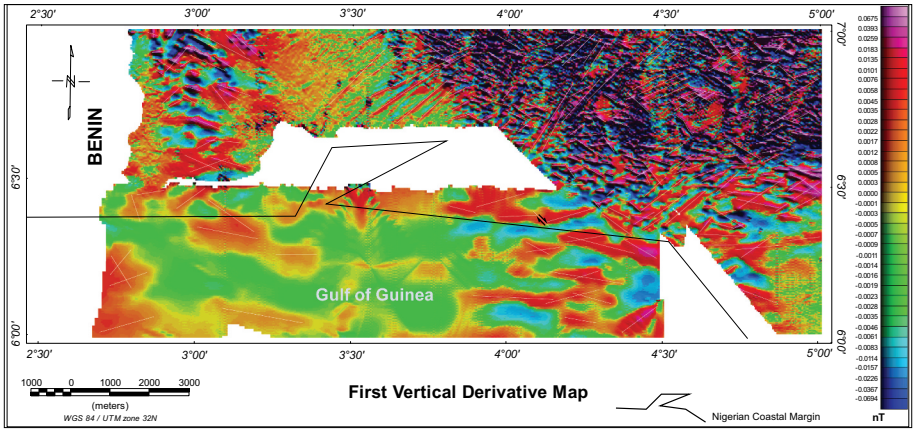

Figure 9. First vertical derivative map showing the shallow faults and lineaments in the study area.

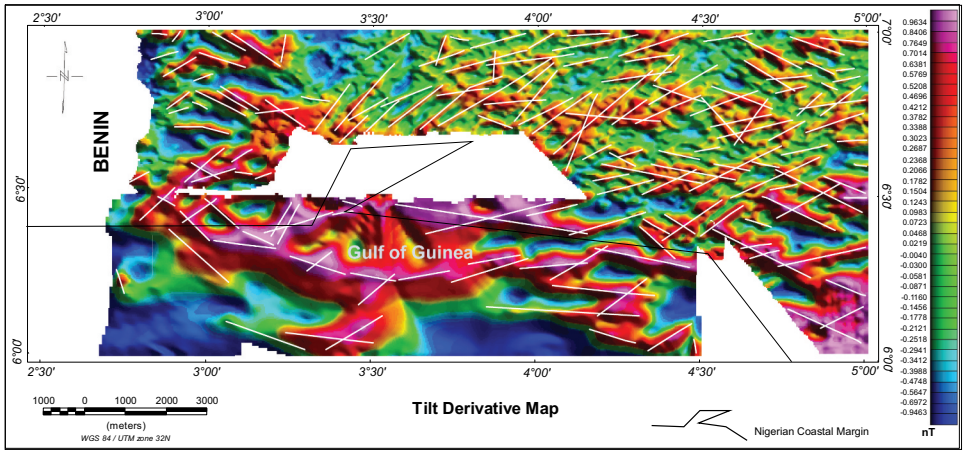

Figure 10. Tilt derivative map showing the delineated subtle faults and lineaments in the study area.

and TDR maps show similarity in locating the contacts and edges of lineaments and were highly suitable for delineating shallow basement structures in the study area. Subtle anomalies not clearly seen on the FVD and THDR maps were better resolved on the TDR map. The identified fault patterns in the study area gave clue to their origin. The NNE-SSW and NE-SW trending faults have been characterised to be the basement bounding faults because of their similarity to those of the oceanic fracture zones that extended into the basin from the Atlantic Ocean (Oluyide 1988; Kaki et al. 2013; Oladele et al. 2015). As the basin evolved through different tectonic episodes, the NW-SE and WNW-ESE trending faults were formed (Oladele et al. 2016).

4.2.2. Deep-seated structures

Deep-seated linear features were identified on the total horizontal derivative of upward continuation (10 km) map, with major trend in the NNE-SSW direction (Figure 11). These structures reflect deep-seated ancient zones of crustal weakness that influenced the structural development of the basin during the Late Jurassic break-up of the Gondwana Super-continent as observed by Oluyide (1988) and Onuoha and Ofoegbu (1988). The faults showed evidence of conjugate sinistral and dextral displacements, which suggests that they are products of the Early Cretaceous transtensional forces associated with the rifting phase that formed the Dahomey Basin (Mascle and Blarez 1987; Antobreh et al. 2009; Nemčok et al. 2012; Davison et al. 2015; Mustapha et al. 2019). The wrench-related movements along oceanic fracture zones could be traced into the Gulf of Guinea (Fairhead 1988; Guiraud et al. 1992; Fairhead et al. 2012). One major NE-SW trending fault was clearly traced into the Atlantic Ocean. This fault could possibly be the continental expression of the Chain Fracture Zone (Okitipupa High), which marks the eastern boundary of the Dahomey Basin (Oladele et al. 2016). Eze et al. (2011) believe that the overprinting relationship between the conjugate wrench faults suggests that the NW-SE trending fault systems post-date the NE-SW fault systems. The NW-SE faults reflect the present-day compressional stress regime acting on the basin due to the tectonic interaction between Africa and Euro-Asian Plates (Fairhead et al. 2013). Transtensional rift phase during the Early Cretaceous opening of the Gulf of Guinea created deep (4–6 km) graben structures filled with non-marine syn-rift sediments along the Romanche Fracture Zone in the

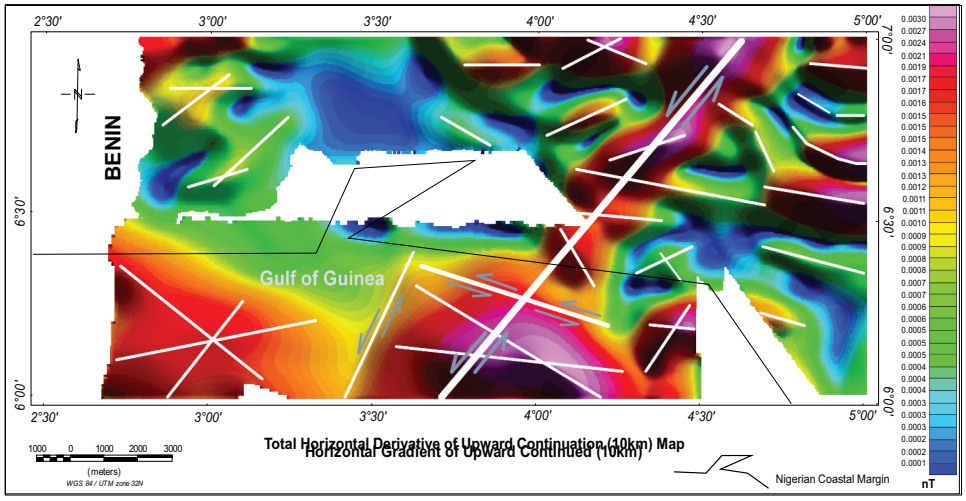

Figure 11. Total horizontal derivative of Upward Continuation (10 km) map showing the delineated Deep-seated faults.

Togo-Benin (Dahomey) Basin (Azevedo 1987; Mascle et al. 1988; Matos 2000). Hence, hydrocarbon prospectivity in the Dahomey Basin would be more rewarding if further exploration efforts are focused towards the offshore areas.

4.2.3. Lineaments analysis, tectonic trends and regional stress-field direction

The geology and tectonics of the Dahomey Basin have been influenced by the Late Jurassic geodynamics that created the Gulf of Guinea, as Africa separated from the South America (Fairhead 1988; Guiraud et al. 1992; Genik 1993). Lineaments mapping and analysis from the first vertical derivative, tilt derivative and total horizontal derivative of upward continued (10 km) maps showed that the area is characterised by shallow and deep-seated regional features reflecting the basement responses to various tectonic episodes that have impacted the basin over time (Semere and Woldai 2006). Rose plots (Figure 12) enabled definition of the dominant structural trends in the basin, and their possible link with transcurrent motions along the oceanic transform faults within the Gulf of Guinea (Mustapha et al. 2019).

Several authors (e.g. Cloetingh and Burov 2011; Fairhead et al. 2013; Gaina et al. 2013) have noted

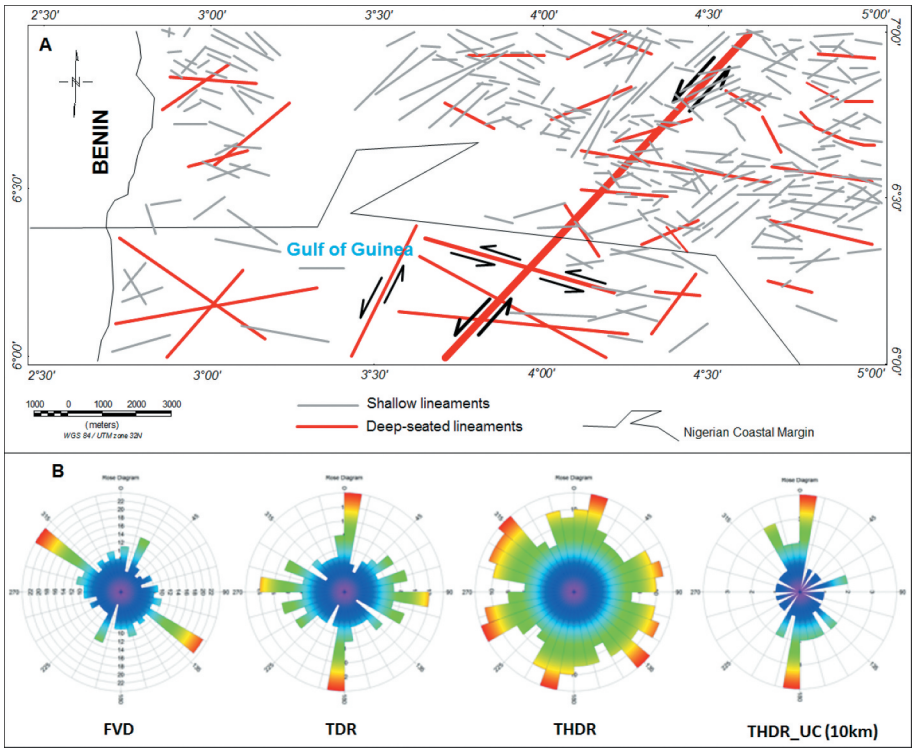

Figure 12. (A) Shallow and deep-seated lineaments in the study area. (B) Rose diagrams show major structural trends in the basin from first vertical derivative (FVD) map, tilt derivative (TDR) map, total horizontal derivative (THDR) map and total horizontal derivative of upward continuation (THDR_UC 10 km) map.

that the development of Mesozoic rift basins in Africa can be associated with movements of old cratonic units in the continental interior and to global tectonics at plate boundaries or to mantle activities (Heine et al. 2008). Stress-related changes at plate boundaries (far-field stresses) could be propagated through the lithospheric plates over long distances (Fairhead et al. 2013; Gaina et al. 2013). This may cause rifting or folding in the continental interior or may lead to changes in basin subsidence rate (Xie and Heller 2009; Fairhead et al. 2012). Furthermore, geometric changes in plate interactions along oceanic transform faults control the rate of movement and orientation of the African cratons. Hence, the geodynamics of the oceanic fracture zones has been responsible for the structural development of rift basins along the West African coast (Fairhead et al. 2012). Furthermore, local changes in intra-cratonic movements within the African Plate affect the stress-field direction, with resultant crustal deformations and changes in the fault geometries of rifted passive margin (Meijer and Wortel 1999; Fairhead et al. 2013).

The mapped deep-seated and near-surface structures in the study area showed strong trends in the NNE-SSW, NE-SW, NW-SE and WNW-ESE directions, respectively. These trends were the products of major structural adjustments of the underlying basement following different extensional and compressional regimes that have shaped and re-shaped the basin from Mesozoic to Recent geologic time (Fairhead et al. 2012) The NNE-SSW and NE-SW trends are contemporaneous with the Early Cretaceous extensional and transtensional forces that acted on oceanic fracture zones and produced deep half-graben structures along the West African Margin (Davison et al. 2015).

The NW-SE and WNW-ESE trends are attributed to basement re-adjustments to compressional activities in the Late Albian-Cenomanian along the Equatorial Atlantic Margin (Benkhelil et al. 1998), the Santonian compressional event mainly pronounced in the Lower Benue Trough (Benkhelil et al. 1998) and far-field stresses (Fairhead et al. 2013) resulting from the compressional interaction between Africa and Euro-Asian Plates (Teasdale et al. 2001; Eze et al. 2011). The far-field stress may have been transmitted to the Dahomey Basin through the West and Central African Rift System which is the weakest link within the African Continent (Fairhead et al. 2013). The overall change in structural trend observed mainly in the near-surface features suggests that the NW-SE and WNW-ESE trending faults postdate the NNE-SSW and NE-SW fault systems (Oladele et al. 2016). This observation emphasises the importance of far-field stress regimes in the structural development of rift basins along passive margins (Abadi et al. 2008; Gaina et al. 2013).

4.3. Depth to basement and sub-basin identification

Determination of depth to magnetic sources using the standard Euler deconvolution and Source Parameter Imaging (SPI) methods showed variations in basement depth varied across the basin. A depth range of 0.1–2.5km was estimated from the standard Euler solutions, while the SPI depth map revealed a rugged basement topography with depth ranges between 0.3km and 6.3km. The map delineated major basement depressions in the offshore part of the basin, ranging in depth from 4.5km to 6.3km. These depth values represent the sedimentary thickness in the study area.

Two sub-basins, "Graben-1" and "Graben-2", were delineated from the SPI map (Figure 13). The sub-basins are separated by a basement uplift (horst block) and are situated at the western and central portions of the offshore Dahomey Basin. The horst structure may have significant effect on the hydrocarbon trap styles and mechanism in the study area by enhancing the formation of 4-way dip closures and other structural traps. The roughly rectangular-shaped "Graben-1" sub-basin is characterised by the presence of small grabens and horsts within grabens, typical of rotated or tilted fault blocks and half-grabens; while the edges of the channel-shaped "Graben-2" becomes broader moving into the ocean basin. The sub-basins are progressively deeper into the Atlantic Ocean, with regional tilt towards the southeast. The structural configuration of "Graben-2" sub-basin suggests that this basement depression may have controlled the creation of the Avon Canyon – an offshore channel through which continental sediments are transported to deep-waters in the Gulf of Guinea (Olabode and Adekoya 2007). The formation of "Graben-2" structure may have also influenced sea water influx from the Atlantic Ocean onto the continent and subsequent flooding of parts of southwestern Nigeria in the present-day Lagos Lagoon.

It is important to mention that most parts of the sub-basins mapped in this study are not yet tested by the drill bit. "Graben-1" plays host to Aje and Ogo Fields offshore Lagos, in which fewer than twenty exploration and appraisal wells have been drilled till date. Hence, offshore Dahomey Basin offers greater promises and higher prospects for

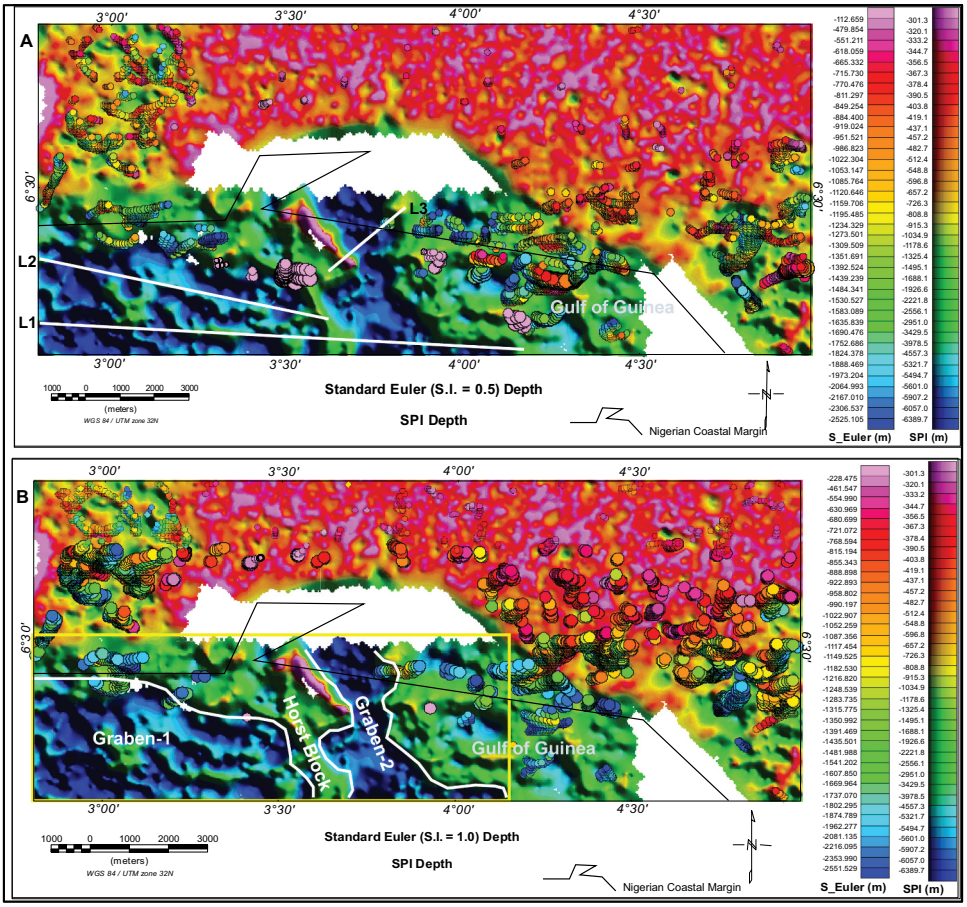

Figure 13. Depth to basement maps of Standard Euler solutions overlaid on the SPI map. (A) Standard Euler solution (S.I. = 0.5) and SPI. (B) Standard Euler solution (S.I. = 1.0) and SPI. The identified sub-basins are enclosed within yellow rectangle; while the white lines labelled L1, L2 and L3 are the modelled profiles across the sub-basins.

finding more conventional oil and gas deposits to boost Nigeria's depleting reserves. Launching drilling campaigns to test the potentials of the Lower Cretaceous sequences in the sub-basins could open-up new opportunities and unlock the undiscovered resources in the basin.

4.4. Basement relief, block pattern and architecture

Insights on the basement relief, block pattern and architecture were obtained from 3D SPI map (Figure 14), in combination with the interpreted aeromagnetic signatures of the study area and 2D forward modelling of selected profiles across the sub-basins. The 3D SPI map gave a robust image of the basement topography and was suitable for understanding the controls on the basin architecture.

Variations in potential field attributes describe basement block pattern and its surrounding features, including faults and lineaments which show strong magnetic expressions (Li et al. 2005). The alternation of high and low aeromagnetic signatures observed on

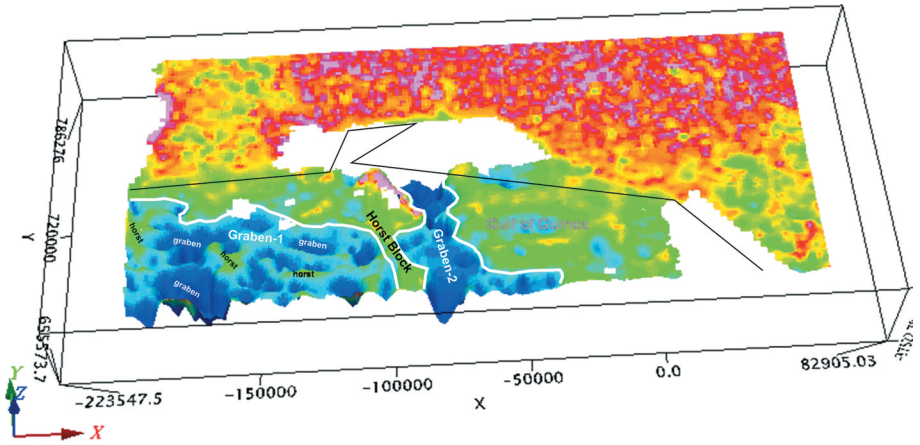

Figure 14. 3D representation of the SPI map showing the basement relief and block pattern in the study area.

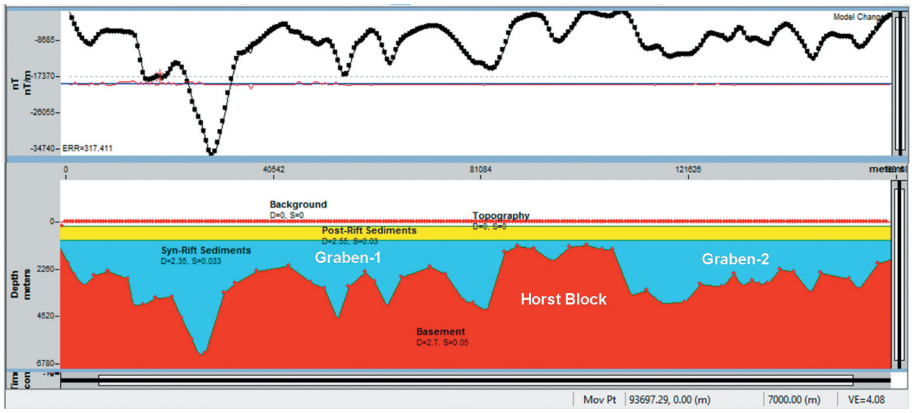

Figure 15. Profile L1 across the sub-basins showing the horst-graben architecture of the basement.

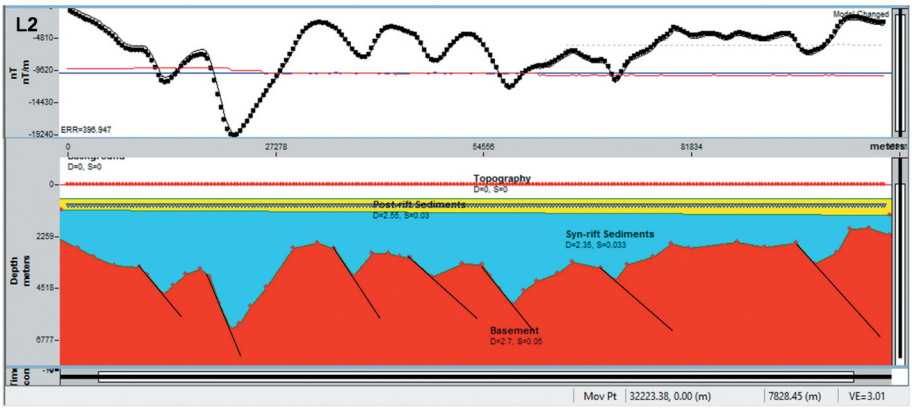

Figure 16. Profile L2 drawn across Graben-1 showing the tilted fault blocks and half-graben structures.

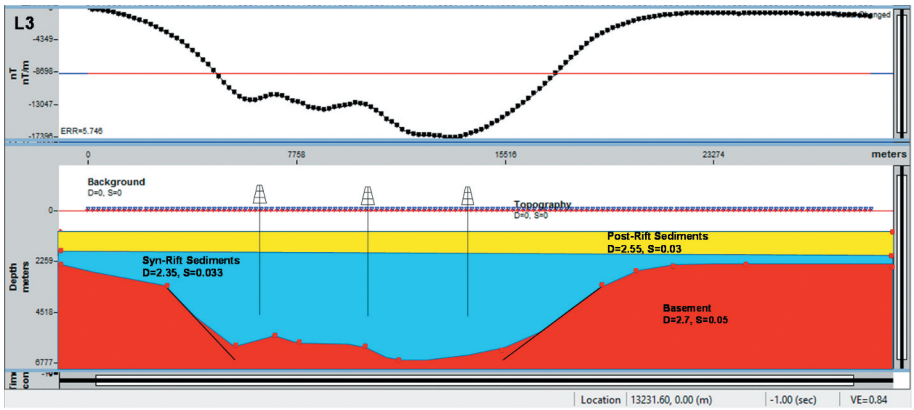

Figure 17. Profile L3 drawn across the channel-shaped Graben-2 showing the untested syn-rift sediments.

the residual map suggested basement high (horst) and low (graben). High magnetic anomalies on the RTE map also reflect regions with high magnetite content (crystalline basement), while regions with low magnetic anomaly suggest areas with relatively low magnetite content (Okpoli and Ekere 2017). These variations reflect the block pattern and rugose morphology of the underlying basement rocks. The interpreted high and low magnetic responses indicate high susceptibility basement uplift and low susceptibility sediment-filled depression, respectively. Major trends of the mapped near-surface and deep-seated structures are in the NNE-SSW, NE-SW, NW-SE and WNW-ESE directions, reflecting their processes of formation. The combination of these structures imposed a horst – graben architecture on the underlying basement rocks in the basin.

The modelled 2D profiles across "Graben-1" and "Graben-2" revealed that the morphology of the basement has been influenced by such processes as block faulting, tilting and rotation (Figures 15, 16 and 17). The basement block pattern largely controlled the basement relief, which in turn affected the near-surface structures and possibly the overlying

stratigraphy. Thus, the basement block pattern and architecture have a direct link to the basin's tectono-stratigraphic history, petroleum systems elements distribution and trapping mechanism. The horst blocks enhance the formation of anticlinal closures and fault dependent traps, while the source-rocks, reservoirs and seal facies are deposited in the grabens. Variations in sedimentary facies will result in the formation of stratigraphic traps, with the faults acting as migration pathways for the generated hydrocarbons.

5. Conclusion

The robust application of high-resolution aeromagnetic data in providing enhanced images of subsurface geological features, basement architecture and sedimentary thickness in the Dahomey Basin have been demonstrated in this study.

Aeromagnetic expressions of the study area showed alternations in high and low anomalies, indicating variations in magnetic susceptibility of the underlying basement and sedimentary rocks. Interpretation of near-surface and deep-seated features revealed that the area is characterised by wrench-related fault systems, with major trends in the NNE-SSW, NE-SW, NW-SE and WNW-ESE directions, respectively. The faults gave clue to their tectono-genesis in relation to the structural development of the Dahomey Basin and the Gulf of Guinea.

Sedimentary thicknesses were found to vary across the basin. The standard Euler solution and SPI methods gave depth ranges of 0.1 km – 2.5 km and 0.3 km – 6.3 km, respectively, for the shallow and deeper magnetic sources. The depth range of 4.5–6.3 km obtained for the two major basement depressions in the offshore part of the Dahomey Basin, provides evidence for the existence of two sub-basins identified in this study simply as Graben-1 and Graben-2. The basement-sediment interface exhibits a horst-graben architecture, which has been controlled by the presence of tilted and rotated fault blocks. The architecture of the basement could be related to the tectono-stratigraphic evolution of the basin, including the formation and distribution of petroleum systems elements and trap styles. While the horst blocks may be responsible for the formation of structural traps, the grabens will host the source rocks, reservoirs and seals. Facies variations will result in stratigraphic traps, with the faults acting as pathways for hydrocarbon migration into the traps. The offshore portion of the basin is adjudged to be deep enough to accommodate thicker sediments with sufficient depths of burial for thermal maturation of organic matter. It will make more sense to have exploration efforts concentrated in the highly prospective offshore portion of the basin. Launching drilling campaigns to test the potentials of the Lower Cretaceous syn-rift plays in the sub-basins could open up new opportunities and throw more light on the structural framework and hydrocarbon prospectivity of the basin.

Acknowledgements

The authors appreciate the input and suggestions made by two anonymous reviewers, which have significantly improved the quality of the manuscript.

Disclosure statement

No potential conflict of interest was reported by the authors.

ORCID

Okoro E. Martins http://orcid.org/0000-0002-8387-8489
Oha A. Ifeanyi http://orcid.org/0000-0002-5465-2114

References

Abadi AM, van Wees J-D, van Dijk PM, Cloetingh SAPL. 2008. Tectonics and subsidence evolution of the Sirt Basin, Libya. Am Assoc Pet Geol Bull. 92(8):993–1027. doi:10.1306/03310806070.

Adekeye OA, Akande SO, Adeoye JA. 2019. The assessment of potential source rocks of Maastrichtian Araromi formation in Araromi and Gbekebo wells Dahomey Basin, southwestern Nigeria. Heliyon, https://doi.org/10.1016/j.heliyon.2019.e01561:1–9.

Adeoye JA, Akande SO, Adekeye OA. 2013. The Cenomanian-Turonian Successions in the Benue Trough and Dahomey Basin, Nigeria: Petroleum Potential Evaluation from New Source Rock Data. NAPE Proceedings of the 30th Annual International Conference and Exhibition, November 11-15 2012, 90-93.

Akande SO, Adekeye OA, Adeoye JA, Jacob N, Lufadeju G 2012. Paleoecologic and organic geochemical assessment of cretaceous hydrocarbon source rocks in the gulf of guinea: new insights from eastern dahomey and benue rift basins with implications for the cenomanian-coniacian petroleum system. Extended Abstract, AAPG Annual Convention and Exhibition, Long Beach, California. 1–10.

Akande SO, Adekeye OA, Adeoye JA, Ojo OJ, Adeoye MO, Dominic W, Erdtmann BD. 2018. Burial and Thermal History of Cretaceous Sediments in the Dahomey, Anambra and Gongola Rift Basins: Implications for Coal Facies Distribution and Petroleum Potential. FUOYE J Pure App Sci. 3(1):308-325.

Antobreh AA, Faleide JI, Tsikalas F, Planke S. 2009. Rift–shear architecture and tectonic development of the Ghana margin deduced from multichannel seismic reflection and potential field data. Mar Pet Geol. 26 (3):345–368. doi:10.1016/j.marpetgeo.2008.04.005.

Azevedo, RP. 1987. Bacia de Barreirinhas: Um Rift Não Convencional. In: 'Rifts' Intracontinentais. Internal Workshop, Petrobras, Rio de Janeiro, Brazil. 140–159.

Babangida J, Olotu S, Ladipo K, Ogunleye M, George CF, Jonathan AE, Okuboyejo A, Oladipo O. 2019. The Structure and Hydrocarbon Prospectivity of the Lower Cretaceous offshore Dahomey Basin, West Africa: A New Syn-rift Half-Graben Frontier Exploration Play in

Nigeria. *NAPE 37th Annual International Conference and Exhibition, Victoria Island Lagos Nigeria. Book of Abstracts and Conference Proceedings*. 159.

Benkhelil J, Mascle J, Guiraud M. 1998. Sedimentary and Structural Characteristics of the Cretaceous Along the Côte D'Ivoire-Ghana Transform Margin and In the Benue Trough: A Comparison 1. In: Mascle J, Lohmann GP, Moullade M. (Eds.). *1998 Proceedings of the Ocean Drilling Program, Scientific Results,* College Station, TX (Ocean Drilling Program) 159:93-99.

Billman HG. 1992. Offshore stratigraphy and paleontology of the Dahomey (Benin) Embayment. NAPE Bull. 70 (2):121–130.

Blakely RJ. 1995. *Potential Theory in Gravity and Magnetic Applications (Cambridge 757 University Press)*. Published by the press syndicate of the University of Cambridge, UK. 81-87.

Brownfield ME, Charpentier RR. 2006. Geology and Total Petroleum Systems of the Gulf of Guinea Province of West Africa. USGS Bull. 2207-C:1–31.

Bumby AJ, Guiraud R. 2005. The Geodynamic Setting of the Phanerozoic Basins of Africa. J Afr Earth Sci. 43(1–3):1–-12. doi:10.1016/j.jafrearsci.2005.07.016.

Burke K, MaCgregor DS, Cameron NR. 2003. In: Arthur TJ, DSN M, Cameron NR, Ed. Petroleum Geology of Africa: new Themes and Developing Technologies. Vol. 207. Geological Society (London): Special Publications; p. 21–60.

Cloetingh S, Burov E. 2011. Lithospheric folding and sedimentary basin evolution: a review and analysis of formation mechanisms. Basin Res. 23(3):257–290. doi:10.1111/j.1365-2117.2010.00490.x.

Cooper GRJ, Cowan DR. 2008. Edge enhancement of potential-field data using normalized statistics. Geophysics. 73(3):1–4. doi:10.1190/1.2837309.

Cordell L, Grauch VJS. 1985. Mapping basement magnetisation zones from aeromagnetic data in the San Juan basin, New Mexico. In: Hinze WJ, editor. The Utility of Regional Gravity and Magnetic Anomaly Maps. Tulsa (OK, USA): Society of Exploration Geophysicists; p. 181–197.

d'Almeida GAF, Kaki C, Adeoye JA, d'Almeida GAF, Kaki C, Adeoye JA. 2016. Benin and Western Nigeria Offshore Basins: a Stratigraphic Nomenclature Comparison. Int J Geosci. 7(02):177–188. doi:10.4236/ijg.2016.72014

Davison I, Faull T, Greenhalgh J, Beirne EO, Ian S. 2015. Transpressional structures and hydrocarbon potential along the Romanche Fracture Zone: a review. In: Nemčok, editor. Transform Margins: development, Controls and Petroleum Systems. Vol. 431. Geological Society (London): Special Publications; p. 1–14.

Eze CL, Sunday VN, Ugwu SA, Uko ED, Ngah SA. 2011. Mechanical Model for Nigerian Intraplate Earth Tremors. 1-6. http://earthzine.org/2011/05/17/mechanical-model-for-nigerian-intraplate-earth-tremors/

Fadiya S, Ojoawo EA. 2015. Foraminiferal Biostratigraphy and Paleoenvironmental Analyses of Sediments from Folu-1 Borehole, Ibeju-Lekki, Lagos State, Nigeria. Ife J Sci. 17:477–492.

Fairhead JD. 1988. Mesozoic plate tectonic reconstructions of the central South Atlantic Ocean: the role of the West and Central African rift system. Tectonophysics. 155(1–-4):181–191. doi:10.1016/0040-1951(88)90265-X.

Fairhead JD, Green CM, Masterton SM, Guiraud R. 2013. The role that plate tectonics, inferred stress changes and stratigraphic unconformities have on the evolution of the West and Central African Rift System and the Atlantic continental margins. Tectonophysics. 594:118–127. doi:10.1016/j.tecto.2013.03.021.

Fairhead JD, Mazur S, Green CM, Masterton S, Yousif ME. 2012. Regional plate tectonic controls on the evolution of the West and Central African rift system, with a focus on the Muglad Rift Basin, Sudan SAPEG. J Sudanese Assoc Pet Geosci. 3:14–29.

Gaina C, Trond HT, van Hinsbergen DJJ, Sergei M, Werner SC, Labails C. 2013. The African Plate: a history of oceanic crust accretion and subduction since the Jurassic. Tectonophysics. 604:4–25.

Genik GJ. 1993. Petroleum Geology of cretaceous–tertiary rift basins in Niger, Chad, and Central African Republic. Am Assoc Pet Geologists Bull. 77:1405–1434.

Geosoft. 2015. Magmap filtering how to guide: defining and applying filters and inverse fft in MAGMAP. Oasis Montaj User Guide, www.geosoft.com:1-23.

Guiraud R, Binks RM, Fairhead JD, Wilson M. 1992. Chronology and geodynamic setting of Cretaceous-Cenozoic rifting in West and Central Africa. Tectonophysics. 213(1–2):227–234. doi:10.1016/0040-1951(92)90260-D.

Guiraud R, Maurin J-C. 1992. Early Cretaceous rifts of Western and Central Africa: an overview. Tectonophysics. 213(1–2):153–168. doi:10.1016/0040-1951(92)90256-6.

Heine C, Muller RD, Steinberger B, Torsvik TH. 2008. Subsidence in intracontinental basins due to dynamic topography. Phys Earth Planet Inter. 171(1–4):252–264. doi:10.1016/j.pepi.2008.05.008.

Ibraheem IM, Elawadi EA, El-Qady GM. 2018. Structural interpretation of aeromagnetic data for the Wadi El Natrun area, northwestern desert, Egypt. J Afr Earth Sci. 139:14–25. doi:10.1016/j.jafrearsci.2017.11.036.

Jan Duchene R. 1998. Geology and Sequence Stratigraphy of the Benin Basin. Report ABACAN. 1–68p.

Kaki C, d'Almeida GAF, Yalo N, Amelina S. 2013. Geology and petroleum systems of the Offshore Benin Basin (Benin). Oil & Gas Science and Technology – Revue d'IFP Energies Nouvelles. 68(2):363–381. doi:10.2516/ogst/2012038.

Ladipo KO, Lipede A 2019. The Frontier Inland Basins of Nigeria: Strategies to realise the significant undiscovered potential. Extended Abstracts, NAPE Special Workshop on Cretaceous Basins in Nigeria, NAF Conference Center Abuja Nigeria. 22-27.

Li J, Morozov I. 2015. 3D aeromagnetic mapping of the Williston Basin Basement. Search Discovery Article #. 41588:1–8.

Li J, Morozov I, Chubak G. 2005. Potential-field Investigation of the Williston Basin Basement. In: Gilboy CF et al. Summary of investigations. Vol. 1. Sask: Geol. Survey, Sask. Industry Resources, Paper A-5; p. 1–11.

Lyatsky HV, Pana DI, Grobe M. 2005. Basement structure in central and southern alberta: insights from gravity and magnetic maps. EUB/AGS Special Rep. 72:1–76.

Mascle J, Blarez E. 1987. Evidence for transform margin evolution from the Ivory Coast – Ghana continental margin. Nature 326:376–381.

Mascle J, Blarez E, Marinho M. 1988. The shallow structures of the Guinea and Ivory Coast-Ghana transform margins: their bearing on the Equatorial Atlantic Mesozoic evolution. Tectonophysics. 155(1–4):193–209. doi:10.1016/0040-1951(88)90266-1.

Matos RMD. 2000. Tectonic evolution of the equatorial South Atlantic. In: Mohriak W, Talwani M. (eds),

Atlantic Rifts and Continental Margins. American Geophysical Union Washington DC, Geophysical Monograph Series. 115:1-32.
McCurry P. 1970. The geology of degree sheet 21. Zaria (Nigeria): Ahmadu Bello University.
Meijer PT, Wortel MJR. 1999. Cenozoic dynamics of the African plate with emphasis on the Africa-Eurasia collision. Journal of Geophysical Research: Solid Earth. 104(B4):7405–7418. doi:10.1029/1999JB900009.
Mekonnen TK. 2004. Interpretation and Geodatabase of Dykes using Aeromagnetic data of Zimbabwe and Mozambique. Unpublished MSc Thesis Applied Geophysics, International Institute for Geo-information Science and Earth Observation Enschede, the Nethrelands. 1-80.
Miller HG, Singh V. 1994. Potential field tilt—a new concept for location of potential field sources. Journal of Applied Geophysics. 32(2–3):213–217. doi:10.1016/0926-9851(94)90022-1.
Milligan PR, Gunn PJ. 1997. Enhancement and presentation of airborne geophysical data. AGSO J Aust Geol Geophys. 17(2):63–75.
Mustapha M, Amponsah P, Bernard P, Bekoa A. 2019. Active Transform Faults in the Gulf of Guinea: Insights from geophysical data and implications for seismic hazard assessment. Can. J. Earth Sci. 56(12):1398–1408.
Nabighian MN, Grauch VJS, Hansen RO, LaFehr TR, Li Y, Peirce JW, Phillips JD, Ruder ME. 2005. The historical development of the magnetic method in exploration. Geophysics. 70(6):33–61. doi:10.1190/1.2133784.
Nemčok M, Henk A, Allen R, Sikora PJ, Stuart C. 2012. Continental break-up along strike slip fault zones; observations from equatorial Atlantic. In: Mohriak WU, Danforth A, Post PJ, Brown DE, Tari GM, Nemčok M, Sinha ST, editors. Conjugate Divergent Margins (Vol. 369). Geological Society (London): Special Publications; p. 537–556.
Okoro EM, Onuoha KM 2019. Structural styles and basement architecture of the dahomey basin from geophysical data. Extended Abstracts, NAPE Special Workshop on Cretaceous Basins in Nigeria. 110–114.
Okpoli CC, Ekere V. 2017. Aeromagnetic mapping of the basement architecture of the Ibadan region, Southwestern Nigeria. Discovery. 53(264):614–635.
Olabode SO, Adekoya JA. 2008. Seismic stratigraphy and development of Avon canyon in Benin (Dahomey) Basin, southwestern Nigeria. J Afr Earth Sci, Elsevier. 50 (5):286–304. doi:10.1016/j.jafrearsci.2007.10.002.
Oladele S, Ayolabi EA. 2014. Geopotential imaging of the benin basin for hydrocarbon prospectivity. NAPE Bull. 26 (1):101–112.
Oladele S, Ayolabi EA, Dublin-Green CO. 2016. Structural characterization of the Nigerian sector of Benin Basin using geopotential field attributes. J Afr Earth Sci, Elsevier. 121:200–209. doi:10.1016/j.jafrearsci.2016.05.021.
Oladele S, Ayolabi EA, Olobaniyi SB, Dublin-Green CO. 2015. Structural features of the benin basin, Southwest Nigeria derived from potential field data. J Mining Geol. 51(2):151–163.
Oluyide PO. 1988. Structural trends in the Nigerian basement complex. In: Oluyide PO, Mbonu WC, Ogezi AE, Egbuniwe IG, Ajibade AC, Umeji AC, editors. Precambrian Geology of Nigeria. Kaduna: Geological Survey of Nigeria; p. 93–98.
Omatsola E 2019. "Why the Cretaceous?" Extended abstracts, NAPE Special Workshop on Cretaceous Basins in Nigeria, NAF Conference Center Abuja Nigeria. 9-14.
Omatsola ME, Adegoke OS. 1981. Tectonic Evolution and Cretaceous Stratigraphy of the Dahomey Basin. Jour Min Geol. 8:30–137.
Omosanya KO, Akinmosin AA, Ikhane PR, Mosuro GO, Goodluck I. 2012. Characterisation of a bitumen seepage in eastern dahomey basin, SW, Nigeria. Adv Appl Sci Res. 3:2078–2089.
Onuoha KM, Ofoegbu CO. 1988. Subsidence and evolution of Nigeria's continental margin: implications of data from Afowo-1 well. Marine Pet Geol. 5(2):175–181. doi:10.1016/0264-8172(88)90022-0.
Opara AI, Ekwe AC, Okereke CN, Nosiri OP. 2012. Integrating airborne magnetic and landsat data for geologic interpretation over part of the Benin basin. Nigeria Pac J Sci Technol. 13(1):556–571.
Oruç B, Keskinsezer A. 2008. Structural setting of the northeastern Biga Peninsula (Turkey) from tilt derivatives of gravity gradient tensors and magnitude of horizontal gravity components. Pure and Applied Geophysics. 165 (9–10):1913–1927. doi:10.1007/s00024-008-0407-8.
Pacino MC, Introcaso A. 1987. Regional anomaly determination using the upwards continuation method. Bolletino Geofísica Teorica Applicada. 29(114):113–122.
Phillips JD 2000. Locating magnetic contacts: A comparison of the horizontal gradient, analytical signal and local wavenumber methods: 70th Annual International Meeting, SEG, Calgary Canada, Expanded Abstracts. 402-405.
Rahaman MA. 1976. Review of the basement geology of southwestern Nigeria. In: Kogbe CA, editor. Geology of Nigeria. Lagos: Elizabethan Publishing Company; p. 41–58.
Reeves CV. 2005. Aeromagnetic Surveys, Principles, Practice and Interpretation. Geosoft. 1–155.
Reid AB, Allsop JM, Granser H, Millet AJ, Somerton IW. 1990. Magnetic interpretation in three dimensions using Euler Deconvolution. Geophysics. 55(1):80–91. doi:10.1190/1.1442774.
Roest WR, Verhoef J, Pilkington M. 1992. Magnetic interpretation using the 3-D analytic signal. Geophysics. 57 (1):116–125. doi:10.1190/1.1443174.
Semere S, Woldai G. 2006. Lineament characterisation and their tectonic significance using Landsat TM data and field studies in the central highlands of Eritrea. J Afr Earth Sci. 46:371–378
Shahverdi M, Namaki L, Montahaei M, Mesbahi F, Basavand M. 2017. Interpretation of magnetic data based on Tilt derivative methods and enhancement of total horizontal gradient, a case study: zanjan Depression. J Earth Space Phys. 43(1):101–113.
Smith RS, Thurston JB, Dai T-F, MacLeod IN. 1998. iSPI ™ — the improved source parameter imaging method. Geophys Prospect. 46(2):141–151. doi:10.1046/j.1365-2478.1998.00084.x.
Solomon S, Ghebreab W. 2006. Lineament characterization and their tectonic significance using Landsat TM data and field studies in the central highlands of Eritrea. J Afr Earth Sci. 46(4):371–378. Elsevier. doi:10.1016/j.jafrearsci.2006.06.007.
Spector A, Grant FS. 1970. Statistical models for interpreting aeromagnetic data. Geophysics. 35(2):293–302. doi:10.1190/1.1440092.
Teasdale J, Lynn P, Mike E, Stuart-Smith P, Loutit T, Zhiqun S, John V, Phil H. 2001. Bass Basin Structurally Enhanced view of Economic Basement (SEEBASE™) Project Report. SRK Consulting, Project Code AG701, Prepared for Geoscience Australia:1-51.

Thompson DT. 1982. EULDPH: a new technique for making computer-assisted depth estimates from magnetic data. Geophysics. 47(1):31–37. doi:10.1190/1.1441278.

Thurston J, Guillion JC, Smith RS 1999. Model independent depth estimation with the SPITM method. 69th Annual International Meeting, SEG, Houston TX, USA. Expanded Abstracts. 403-406.

Thurston JB, Smith RS. 1997. Automatic conversion of magnetic data to depth, dip, and susceptibility contrast using the SPI (^{TM}) method. Geophysics. 62(3):807–813. doi:10.1190/1.1444190.

Tyrrell E, Elliott P, Lofgran M, Biaou B. 2017. The overlooked potential of Devonian, Jurassic, Cretaceous and Tertiary Plays within the onshore and shefal Dahomey Embayment. In: benin, the low-cost high impact frontier. GeoExpro. 14(5):34–37.

Verduzco B, Fairhead JD, Green CM, MacKenzie C. 2004. New insights into magnetic derivatives for structural mapping. The Leading Edge. 23(2):116–119. doi:10.1190/1.1651454.

Xie X, Heller PL. 2009. Plate tectonics and basin subsidence history. Geol Soc Am Bull. 121:55–64.